Soft-input soft-output lattice sphere decoder for linear channels

Joseph Boutros[†], Nicolas Gresset[†⋆], Loïc Brunel[⋆] and Marc Fossorier[†◇]

[†] ENST, 46 Rue Barrault, 75013 Paris, France
[⋆]Mitsubishi Electric ITE-TCL, 1 Allée de Beaulieu, 35700 Rennes, France
[◇]Department of Electrical Engineering, University of Hawaii, Honolulu HI 96822, USA
{boutros,gresset,brunel,fossorier}@enst.fr

***Abstract*— Soft output detection for signals transmitted on linear channels is investigated. A particular emphasis is made for signal detection on multiple antenna channels. The a posteriori information at the detector output is evaluated from a shifted spherical list of point candidates. The spherical list is centered on the maximum likelihood point, which has the great advantage of stabilizing the list size. Thus, the sphere radius is selected in order to control the list size and to cope with the boundaries of the finite multiple antenna constellation. Our new soft output sphere decoder is then applied to the computation of constrained channel capacity and to the iterative detection of a coded transmission. For example, we achieved a signal-to-noise ratio at 1.25dB from capacity limit on a 4×4 MIMO channel with 16-QAM modulation and a 4-state rate 1/2 parallel turbo code.**

I. Introduction

In order to improve the data transmission rate over fading channels, most of recent systems use a set of multiple antennas [9][15] for transmitting and receiving. Iterative a posteriori probability (APP) techniques [2][11], such as iterative joint detection and decoding [3][4], are a judicious choice for high performance receivers with reasonable complexity. Such techniques require soft-input soft-output detectors and decoders. Soft-output detection on multiple antenna (MIMO) channels can be achieved via an exhaustive list as in [3] or a limited size list of a spherical shape as in [10]. The APP detector based on an exhaustive list has a relatively large complexity, exponential in the number of transmit antennas and the number of bits per modulation symbol. On the contrary, an APP detector based on a non-exhaustive list is sub-optimal but its complexity is proportional to the list size. The main weak point in the spherical list decoder already proposed is the instability of the list size and the associated problem of sphere radius selection. In this paper, we propose a new soft-output lattice decoder applicable to all linear channels including multiple antennas. Our APP detector starts by applying an accelerated sphere decoder to find the maximum likelihood (ML) point. Then, using a double Pohst recursion, it builds a spherical list centered around the ML point (not the received point!) to evaluate channel likelihoods. The effective list size is well controlled and depends on the ML point position and the channel state.

The paper is organized as follows. The channel model is presented in section II. Lattice representation of MIMO channels is given in section III. In section IV, we briefly describe the accelerated sphere decoder that takes into account the finite QAM size. In section V, we present the construction of the shifted spherical list for soft output detection. Finally, two computer simulations are presented in section VI.

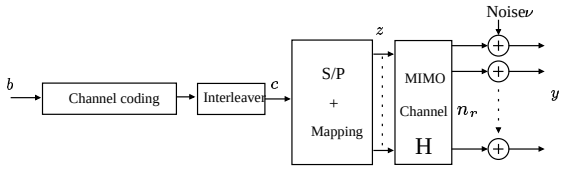

Fig. 1. Transmitter system model.

II. System model and parameters

Lattice theory and coding theory are applied to efficiently encode and decode information in a digital transmission system with multiple antennas. The transmitter structure of a bit interleaved coded modulation (BICM, see [5]) is illustrated in Fig. 1. The information binary elements are encoded by a rate R_c channel code. The coded bits $\{c_\ell\}$ are randomly interleaved and fed to a 2^m-QAM mapper. Information is conveyed on a multiple antenna channel with n_t transmit antennas and n_r receive antennas. It is assumed that $n_t = n_r$ throughout this paper. Channel input and output are linked via the non-selective Rayleigh fading model:

$$y = zH + \nu = x + \nu \tag{1}$$

where $H = [h_{ij}]$ is an $n_t \times n_r$ complex matrix, $z \in \mathbb{C}^{n_t}$ denotes the MIMO channel input, $x \in \mathbb{C}^{n_r}$ the noiseless channel output, $y \in \mathbb{C}^{n_r}$ the MIMO channel output and ν is a white complex Gaussian additive noise with zero mean and variance $2N_0$ per complex component. The entries h_{ij} of the channel matrix are complex random variables with a Gaussian probability distribution of zero mean and unity variance. The spectral efficiency of the illustrated BICM is $R_c \times m \times n_t$ bits per channel use.

III. Lattice representation of MIMO channels

Lattice theory is a powerful mathematical tool to represent the channel geometrically and help us understand its behavior in order to design a good modulator and its corresponding demodulator. Since multi-dimensional QAM constellations are subsets of $\mathbb{Z}^n$, we can write $z \in \mathbb{Z}^{2n_t}$. Let $n_s = 2n_t$ denote the dimension of the real Euclidean space. The equality $x = zH$ is now extended to the real space $\mathbb{R}^{n_s}$ to get

$$x = zM, \quad x \in \mathbb{R}^{n_s}, \quad z \in \mathbb{Z}^{n_s} \tag{2}$$

Therefore, the MIMO channel output $y = x + \nu$ is obtained by perturbing a lattice point x with additive white noise ν. A lattice Λ is a discrete subgroup of $\mathbb{R}^{n_s}$ [7], i.e., it is a $\mathbb{Z}$-module of rank n_s. In (2), the lattice Λ is generated by the $n_s \times n_s$ real matrix $M = [M_{ij}]$ which is derived from the channel matrix H by the following simple relation

$$M_{ij} = \begin{pmatrix} \Re h_{ij} & \Im h_{ij} \\ -\Im h_{ij} & \Re h_{ij} \end{pmatrix} \quad (3)$$

where $\Re h_{ij}$ and $\Im h_{ij}$ denote the real and imaginary part of h_{ij}, respectively. The matrix M is called *lattice generator matrix* [7]. Geometrically, the point x belongs to a discrete infinite set of points satisfying a group structure. When z is restricted to a finite QAM integer constellation, then x belongs to a finite lattice constellation denoted by Ω. With the notations of the previous section, the cardinality of Ω is 2^{mn_t}.

IV. Accelerated sphere decoding algorithm

A maximum likelihood lattice decoder applied to the received point $y = x+\nu$ determines the nearest lattice point to y, i.e., it minimizes $||y - x||$. The main idea of the very efficient sphere decoder algorithm [16][17][1] is to enumerate lattice points inside a sphere centered on y and reduce the radius of the sphere each time a new point is found. This drastically decreases the number of enumerated points but still ensures the closest point criterion. If no point is found, the radius of the search sphere should be enlarged.

The complexity of the sphere decoder depends on many parameters, we cite the enumeration strategy inside the sphere, the lattice structure and the specific lattice basis M used in the quadratic form $||x||^2 = Q(z) = zMM^tz^t$. Two non-trivial lattice decoding strategies are known in the literature:

- *The Sphere Decoder based on Pohst strategy* [13][8] was applied by Viterbo, Biglieri and Boutros (VB) [16][17] to digital communications. The key idea is to enumerate lattice points inside an ellipsoid in the integer space that corresponds to a spherical search region in the real space. The search complexity is sensitive to the choice of the initial radius.
- *The Sphere Decoder based on Schnorr-Euchner strategy* [14] was applied by Agrell, Eriksson, Vardy and Zeger (AEVZ) in [1]. The key idea is to view the lattice as laminated hyperplanes and then start the search for the closest point in the nearest hyperplane. A search radius can be specified in order to limit the search region to a sphere. AEVZ decoding complexity is quasi-insensitive to the choice of the initial radius.

Both sphere decoders (VB and AEVZ) may be accelerated, by a factor up to 10, if M is reduced via KZ or LLL algorithms. These reduction algorithms have a main drawback if the lattice constellation is finite. Indeed, LLL and KZ perform a basis conversion and hence they convert the constellation cube (QAM modulation assumed) into a parallelotope where the boundaries are very difficult to determine. Furthermore, in most practical situations, the complexity decrease obtained by taking into account the finite structure of the constellation is much more profitable than the application of LLL/KZ algorithms. On multiple antenna channels, VB and AEVZ complexities are similar at moderate and high signal-to-noise ratios (SNR). At low SNR, AEVZ may show a speed gain with respect to VB by a factor varying from 1 up to 4. Thus, we propose below a modified version of the AEVZ sphere decoder that takes into account the boundaries of the finite QAM constellation, without including any lattice reduction. This modified AEVZ sphere decoder may be viewed as the extension of the depth-first branch-and-bound algorithm [12].

Accelerated Sphere Decoder: Applying Schnorr-Euchner strategy + taking into account the boundaries of the finite QAM constellation

Input. A received point y, the generator matrix $M(n_s \times n_s)$ of the lattice, the radius R of the sphere, and the bounds z_{min} and z_{max} of the constellation. You can set the radius R to $+\infty$. A slight gain in speed of at most 30% can be obtained if R is linked to the Gaussian noise variance N_0 or to the minimum distance $d_{Emin}(\Lambda)$

Output. The ML point z_{ML} belonging to the constellation and its squared Euclidean distance to y

Step 1. (Pre-processing) Compute the Gram matrix $G = MM^t$ and do a Cholesky decomposition $G = VV^t$, where V is lower-triangular. Compute the inverse $V^I = V^{-1}$

Step 2. (Initialization) Set $bestdist \leftarrow R^2$, $k \leftarrow n_s$, $dist_k \leftarrow 0$, $e_k \leftarrow yM^{-1}$, $z_k \leftarrow [e_{kk}]$, $z_k \leftarrow max(z_k, z_{min})$, $z_k \leftarrow min(z_k, z_{max})$, compute $\rho = (e_{kk} - z_k)/(V^I_{kk})$, $step_k \leftarrow sign(\rho)$

Step 3. Compute $newdist \leftarrow dist_k + \rho^2$. If $newdist < bestdist$ and $k \neq 1$ then go to 4 else go to 5 endif

Step 4. Compute for $i = 1, ..., k-1$ $e_{k-1,i} \leftarrow e_{k,i} - \rho V^I_{ki}$, decrement k, set $dist_k \leftarrow newdist$, $z_k \leftarrow [e_{kk}]$, $z_k \leftarrow max(z_k, z_{min})$, $z_k \leftarrow min(z_k, z_{max})$, $\rho = (e_{kk} - z_k)/(V^I_{kk})$, $step_k \leftarrow sign(\rho)$, go to 3

Step 5. If $newdist < bestdist$ then set $z_{ML} \leftarrow z$, $bestdist \leftarrow newdist$, else if $k = n$ then return z_{ML} and terminate, else increment k, endif. Compute $z_k \leftarrow z_k + step_k$, if $z_k < z_{min}$ or $z_k > z_{max}$ then $step_k \leftarrow -step_k - sign(step_k)$, $z_k \leftarrow z_k + step_k$ endif. If $z_k < z_{min}$ or $z_k > z_{max}$ then go to 5, endif. $\rho \leftarrow (e_{kk} - z_k)/V^I_{kk}$, $step_k \leftarrow -step_k - sign(step_k)$, go to 3

Fig. 2 shows the bit error rate (BER) performance of the accelerated sphere decoder with up to 16 antennas and an uncoded 16-QAM constellation. In the case of 16×16 MIMO, the lattice constellation Ω has 2^{64} points. Even though, the accelerated sphere decoder quickly succeeded in finding the ML point in the whole range $10^{-1}...10^{-6}$ of BER.

V. Construction of a shifted spherical list for soft output lattice decoding

Let c_j denote the j-th coded bit. The index j satisfies $1 \leq j \leq mn_t$ when considering a signal detection associated to one symbol period. The iterative APP detector has two inputs (see Fig. 4 below): The received vector y and the a priori probabilities on the coded bits $\pi(c_j)$. The detector delivers the a posteriori probabilities $APP(c_j)$ and the extrinsic probabilities $\xi(c_j)$.

A. Exhaustive APP detector

Consider the lattice constellation Ω defined in section III. For a given c_j, we can write $\Omega = \Omega(c_j = 0) \cup \Omega(c_j = 1)$. The sub-constellation $\Omega(c_j = 0)$ (resp. $\Omega(c_j = 1)$) is defined by all constellation points where the j-th bit of the binary mapping is

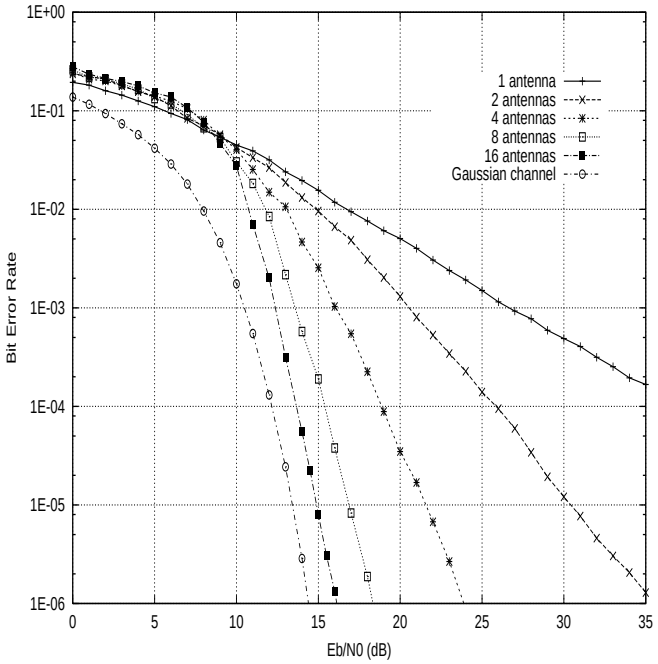

Fig. 2. Bit error rate of a 16-QAM on a flat Rayleigh MIMO channel.

equal to 0 (resp. 1). Then, the extrinsic information delivered by the soft output detector is

$$\xi(c_j) = \frac{\sum_{z' \in \Omega(c_j=1)} \left[\left(e^{-\frac{\|y - z'M\|^2}{2N_0}} \right) \prod_{r \neq j} \pi(c_r) \right]}{\sum_{z \in \Omega} \left[\left(e^{-\frac{\|y - zM\|^2}{2N_0}} \right) \prod_{r \neq j} \pi(c_r) \right]} \quad (4)$$

The above equation is well known in the turbo coding community, we do not give details about its proof due to the lack of space. Equation (4) is the extrinsic probability for $c_j = 1$. As an example, for $n_t = n_r = 4$ and a 16-QAM modulation, (4) requires the computation of 2^{16} likelihoods for each binary element! It is clear that exhaustive APP detection is practically limited to the situations where $mn_t \leq 8$, e.g., two antennas and 16-QAM or four antennas and QPSK.

B. List APP detector

When the product mn_t is large, greater than 8 in practical systems, point enumeration over the whole constellation Ω is replaced by a point enumeration over a reduced size subset $\mathfrak{L} \subset \Omega$, also called *list*. The list size should be small with respect to $|\Omega| = 2^{mn_t}$. We observe that soft outputs depend both on the geometrical configuration when considering the likelihoods, and on the a priori probability configuration fed back from the decoder. In (4), some of the likelihoods are negligible. In the absence of a priori information, let us suppose that all the points with non-negligible likelihood belong to the list $\mathfrak{L}$:

$$\forall z' \notin \mathfrak{L}, \quad \forall z \in \mathfrak{L}, \quad e^{-\frac{\|y - z'M\|^2}{2N_0}} \ll e^{-\frac{\|y - zM\|^2}{2N_0}} \quad (5)$$

Thus, $\mathfrak{L}$ contains lattice points inside a sphere of radius R centered on the received point y. The choice of the sphere radius determines the performance and the complexity of the corresponding soft-in soft-out detector and is the main difficulty encountered in classical list detectors. Also, when $\mathfrak{L}$ is centered on y, the radius R depends largely on the position of y in $\mathbb{R}^{n_s}$, since $\mathfrak{L}$ contains only lattice points belonging to the intersection of the sphere and Ω (see Fig. 3).

C. Our shifted spherical list APP detector

Once the ML point $x_{ML} = z_{ML}M$ is found by an accelerated sphere decoder, we choose to center the spherical list $\mathfrak{L}$ on x_{ML} instead of y. Figure 3 clearly illustrates the advantages of the ML center when compared with the received point center. Indeed, when y is outside the constellation Ω, which occurs at a high probability when considering large number of dimensions, the sphere centered on the received point enumerates a large number of lattice points to find a small number of constellation points. When the sphere is centered on x_{ML}, the number of enumerated points is dramatically reduced and the high likelihood constellation points are taken into account. A double Pohst recursion [13][8][6] is used to enumerate lattice points inside the spherical list. The first classical recursion is needed to check all lattice points at a squared distance less than R^2 from x_{ML}, i.e., solve $Q(z - z_{ML}) = ||x - x_{ML}||^2 \leq R^2$. The second parallel recursion easily evaluates the squared Euclidean distances $||y - zM||^2$ between the enumerated points $x = zM$ and the received point y in order to compute the channel likelihoods.

Shifted spherical list enumeration with a double Pohst recursion

Input. A received point y, a constellation point x_{ML}, the generator matrix $M(n_s \times n_s)$ of the lattice, the radius R of the sphere according to (10) below, and the bounds z_{min} and z_{max} of the constellation

Output. A list $\mathfrak{L}$ of lattice points inside the sphere, a list of squared Euclidean distances between y and each point in the list

Step 1. (Pre-processing) Compute the Gram matrix $G = MM^T$ and do a Cholesky decomposition $G = VV^t$, V is lower-triangular. Cholesky decomposition produces an upper-triangular matrix $Q = [q_{ij}]$, $q_{ii} = V_{ii}^2$, and $q_{ij} = V_{ji}/V_{ii}$ for $i = 1 \ldots n_s$ and $j = i + 1 \ldots n_s$. Compute the inverse M^{-1}, $u = z_{ML} = x_{ML}M^{-1}$ and $\rho = yM^{-1}$. Notice that z_{ML} can be directly offered by the accelerated sphere decoder (section IV).

Step 2. (Initialization) Set $d^2 \leftarrow R^2$, $T_{n_s} \leftarrow R^2$, $T_{n_s}^d \leftarrow R^2$. For $j = 1 \ldots n_s$ set $S_j \leftarrow u_j$, $S_j^d \leftarrow \rho_j$, $i \leftarrow n_s$

Step 3. Compute $L_i \leftarrow min\left(\left\lfloor \sqrt{T_i/q_{ii}} + S_i \right\rfloor, z_{max} \right)$ and $z_i \leftarrow max\left(\left\lceil -\sqrt{T_i/q_{ii}} + S_i \right\rceil, z_{min} \right) - 1$

Step 4. Increment z_i. If $z_i \leq L_i$ if $i > 1$ compute $\xi_i \leftarrow u_i - z_i$ and $\xi_i^d \leftarrow \rho_i - z_i$, compute $T_{i-1} \leftarrow T_i - q_{ii}(S_i - z_i)^2$ and $T_{i-1}^d \leftarrow T_i^d - q_{ii}(S_i^d - z_i)^2$, compute $S_{i-1} \leftarrow u_{i-1} + \sum_{j=i}^{n_s} q_{i-1,j}\xi_j$ and $S_{i-1}^d \leftarrow \rho_{i-1} + \sum_{j=i}^{n_s} q_{i-1,j}\xi_j^d$, decrement i and go to 3, else compute $\hat{d}^2 \leftarrow R^2 - T_i^d + q_{11}(S_1^d - z_1)^2$, store z and $\hat{d}$ in $\mathfrak{L}$, go to 4, endif, else if $i = n_s$ terminate else increment i and go to 4, endif, endif

D. Choice of the shifted list radius R

In this section, some properties of the lattice Λ and the constellation Ω are exploited to determine a sphere radius that guaranties a high stability for the number of points

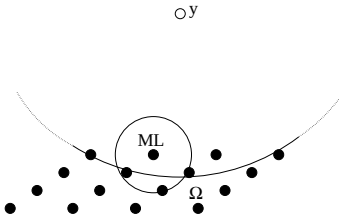

Fig. 3. Comparison between a spherical list centered on the ML point and a spherical list centered on the received point y (low SNR situation).

required in the list. Let us assume that our initial objective is to find N_p points to create a list centered on x_{ML}. We can make the approximation that the volume of a sphere containing N_p points is equal to the volume of N_p fundamental parallelotopes. Hence, the radius R is well approximated by

$$R \approx \left(\frac{N_p \times vol(\Lambda)}{V_{n_s}} \right)^{\frac{1}{n_s}} \tag{6}$$

where $vol(\Lambda) = |det(M)|$ and V_{n_s} is the volume of a unit radius sphere in the real space $\mathbb{R}^{n_s}$, $V_{n_s} = \pi^{n_t}/n_t!$. This method of choosing the radius is quite stable in a lattice when N_p is relatively large. The effective number N_e of points in $\mathfrak{L}$ is very close to the number N_p, or equivalently $N_e/N_p \approx 1$. Now, when considering a finite constellation $\Omega \subset \Lambda$, the intersection between the sphere and the constellation significantly diminishes N_e, depending on the position of the ML point in the constellation Ω and the shape of Ω. Thus, the fraction N_e/N_p should be controlled by taking into account the influence of these two parameters. As an example, consider a cubic integer constellation Ω in $\mathbb{R}^{n_s}$. We can evaluate the average number of points in the list by the simple hypothesis that it is divided by 2 for each dimension where the ML point is on the edge of the constellation. For a 16-QAM with $n_t = n_s/2$ transmit antennas, we have $\mathrm{C}_{n_s}^{i} \times 2^{n_s}$ points with i components on the edge of the constellation. This leads to an average number of points for 16-QAM equal to

$$E[N_e] = \sum_{i=0}^{n_s} \mathrm{C}_{n_s}^{i} . \frac{2^{n_s}}{4^{n_s}.2^{i}} N_p = \left(\frac{3}{4} \right)^{n_s} N_p \tag{7}$$

When $n_t = 4$, the average reduction factor is about $1/10$. Hence, in the general case of a random (non-cubic) constellation Ω given by the MIMO channel, we can adjust the sphere radius by taking into account the number of hyperplanes n_{hyp} at the constellation boundaries passing through the ML point. The number of expected points N_p is multiplied by $\alpha[n_{hyp}]$, an expansion factor of the list size which depends on n_{hyp}. Indeed, the more the number of hyperplanes the ML point belongs to, the less the points in the list. For the special case of MIMO channels family, the empirical choice $\alpha[i] = \lfloor i/2 \rfloor + 1$ yields good results.

The number N_e is also influenced by the shape of Ω. A non-cubic shape with an acute corner attenuates the fraction N_e/N_p. We selected the normalized distance $\gamma(G)$ as a figure of merit for the shape of Ω:

$$\gamma(G) = \frac{d^2_{Emin}(G)}{vol(\Lambda)^{2/n_s}} \tag{8}$$

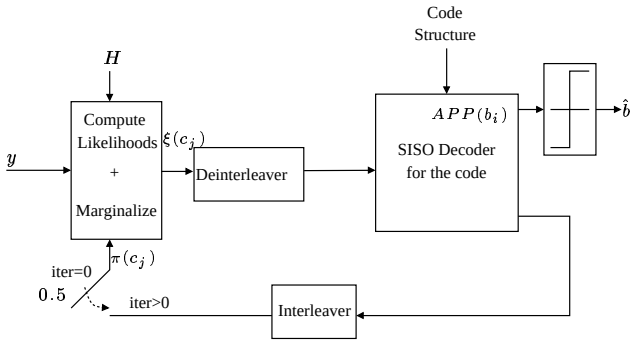

Fig. 4. Iterative detection and decoding.

where $d^2_{Emin}(G)$ is the minimum diagonal element of the Gram matrix G. Then, we introduce an additional expansion factor $\mu_\gamma > 1$ and apply the simple rule:

$$\gamma(G) > \gamma_i \Rightarrow \mu_\gamma = \mu_i \tag{9}$$

In the 8-dimensional real space, one may take $\gamma_1 = 3dB, \gamma_2 = 6dB, \mu_1 = 4$, and $\mu_2 = 16$. Finally, the radius R of the shifted spherical list $\mathfrak{L}$ should be computed according to

$$R = \left(\frac{\alpha[n_{hyp}] \times \mu_\gamma \times N_p \times vol(\Lambda)}{V_{n_s}} \right)^{\frac{1}{n_s}} \tag{10}$$

E. Complexity reduction for block fading channels

In the case of block fading channels, the channel remains unchanged during the block period. Thanks to the lattice group structure, we can find the points in the sphere centered on the origin 0 and then translate them to find the points in the sphere centered on x_{ML}. In the list, we store $N_{\mathfrak{L}}$ points belonging to the constellation with their integer labeling. For each channel use, the additive Gaussian noise moves y, so the distances $||y - zM||$ have to be reprocessed. We can also enumerate a larger list and sort it by increasing distance to the origin. This can be seen as a list of concentric spheres. If the first sphere leads to a list which is too small, then we consider the second sphere and so on.

F. Applications to iterative detection and decoding of BICM

An iterative joint APP detection and decoding receiver is based on the exchange of soft values between the SISO QAM-detector and the SISO channel code decoder. The information exchange between inputs and outputs of the two blocks is shown on Fig. 4. We assume that the reader is familiar with turbo detection and decoding techniques. Figure 5 gives the detailed block diagram of the soft output detector. The reader should notice that the sphere decoder (including the search of x_{ML} and the construction of $\mathfrak{L}$) is outside the iterative detection and decoding loop.

VI. Computer simulations and numerical results

Let us consider a rate $1/2$ parallel turbo code [2] whose constituent codes are two $(1, 5/7)$ recursive systematic convolutional codes. The rate 1/2 constituents are punctured in order to increase the concatenation rate from 1/3 to 1/2. Figure 6 shows the achievable information rate for 4×4 multiple

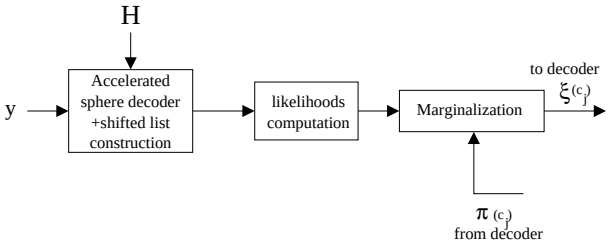

Fig. 5. Detailed blocks of the soft output detection.

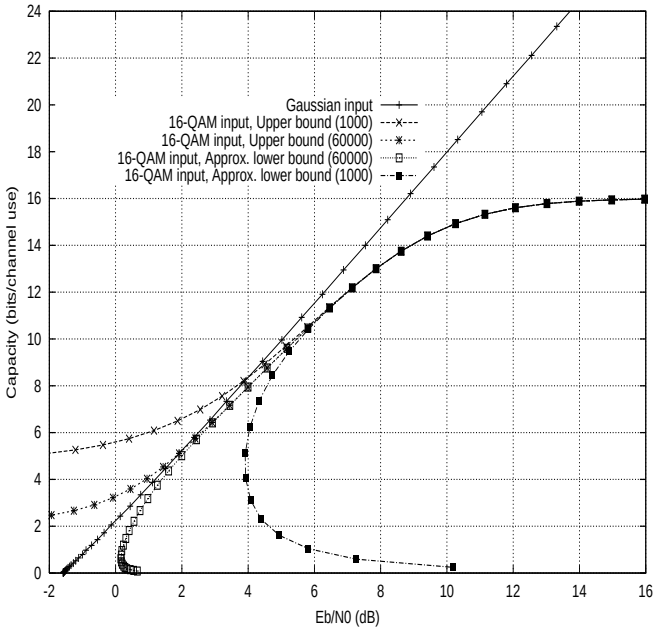

Fig. 6. Achievable rate on a 4×4 ergodic MIMO with 16-QAM input, $N_p = 1000/60000$, $N_e(min) = 256/4000$.

antenna channel with 16-QAM input alphabet. The mutual information value of 8.0 bits per channel use yields a minimum achievable signal-to-noise ratio equal to 4.0dB. The capacity limit with a Gaussian input at 8.0 bits per channel use is 3.7 dB. Figure 6 illustrates an application of the soft output sphere decoder to the evaluation of MIMO channel information rate under the constraint of a finite QAM constellation input. Two scenarios are presented: 1- A target list size $N_p = 1000$. The effective list size was distributed between $N_e(min) = 256$ and $N_e(max) = 2300$ with an average equal to 1000. 2- A target list size $N_p = 60000$! The effective list size was distributed between $N_e(min) = 4000$ and $N_e(max) = 26000$ with an average equal to 10000. It is clear that mutual information evaluation is useful at high coding rates ($R_c \geq 1/2$) where its value diverges from the gaussian input capacity. A reduced size list is sufficient in this region. Figure 7 illustrates the performance of the 4-state parallel turbo code described above. The BICM interleaver size is 20000 and 100000 coded bits respectively. The total number of performed detection/decoding iterations in the BICM receiver is 25. The two different list constructions are also presented, the list centered on y and the list centered on x_{ML}. The performance curve to the most left shows a BER of 10^{-5} at 1.25dB from capacity limit under the constraint of a 16-QAM channel input.

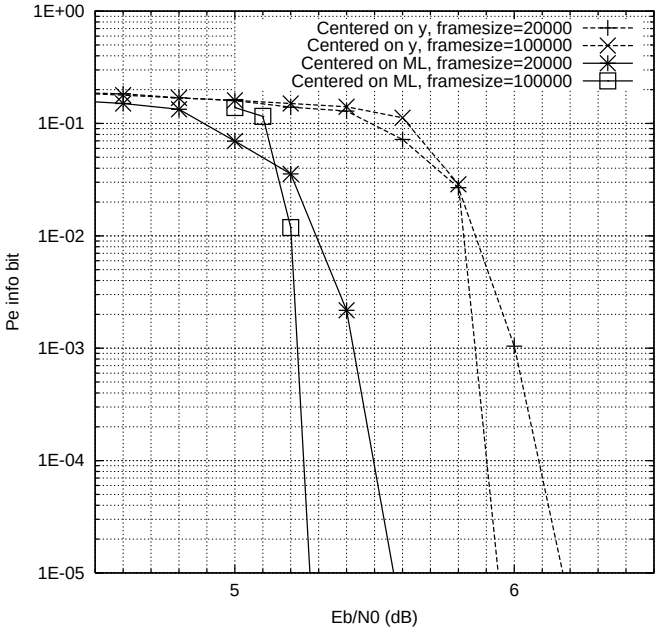

Fig. 7. Performance on 4×4 ergodic MIMO with 16-QAM, rate 1/2 4-state parallel turbo code, $N_p = 3000$ points.

REFERENCES

[1] E. Agrell, T. Eriksson, A. Vardy and K. Zeger, "Closest point search in lattices," *IEEE Trans. on Inf. Theory*, pp. 2201-2214, August 2002.

[2] C. Berrou, A. Glavieux, and P. Thitimajshima, "Near Shannon limit error-correcting coding and decoding: turbo-codes," *Proceedings of ICC'93*, Geneva, pp. 1064-1070, May 1993.

[3] J. Boutros, F. Boixadera and C. Lamy, "Bit-interleaved coded modulations for multiple-input multiple-output channels," *IEEE 6th Int. Symp. on Spread Spectrum Techniques & App.*, NJ, September 2000.

[4] J. Boutros and G. Caire, "Iterative multiuser joint decoding: unifi ed framework and asymptotic analysis," *IEEE Trans. on Inf. Theory*, vol. 8, pp. 1772-1793, July 2002.

[5] G. Caire, G. Taricco, E. Biglieri, "Bit-interleaved coded modulation," *IEEE Trans. on Inf. Theory*, vol. 44, no. 3, May 1998.

[6] Henri Cohen: *Computational algebraic number theory*, Springer Verlag, 1993.

[7] J. H. Conway, N. J. Sloane, "Sphere packings, lattices and groups," 3rd edition, 1998, Springer-Verlag, New York.

[8] U. Fincke and M. Pohst, "Improved methods for calculating vectors of short length in a lattice, including a complexity analysis," *Mathematics of Computation*, vol. 44, pp. 463-471, April 1985.

[9] G.J. Foschini, Jr. and M.J. Gans, "On limits of wireless communication in a fading environment when using multiple antennas," *Wireless Personal Communications*, vol. 6, no. 3, pp. 311-335, March 1998.

[10] B. Hochwald and S. ten Brink, "Achieving near-capacity on a multiple-antenna channel," submitted to the *IEEE Transactions on Communications*, July 2001.

[11] F. Kschischang, B. Frey, H.-A. Loeliger, "Factor graphs and the sum-product algorithm," *IEEE Transactions on Inf. Theory*, vol. 47, no. 2, February 2001.

[12] J. Luo, K. Pattipati, P. Willett, L. Brunel, "Branch-and-bound-based fast optimal algorithm for multiuser detection in synchronous CDMA," *IEEE International Conference on Communications*, Anchorage, May 2003.

[13] M. Pohst, "On the computation of lattice vectors of minimal length, successive minima and reduced bases with applications," *ACM SIGSAM Bull.*, vol. 15, pp.37-44, 1981.

[14] C.P. Schnorr and M. Euchnerr, "Lattice basis reduction: improved practical algorithms and solving subset sum problems," *Mathematical Programming*, vol.66, pp.181-191, 1994.

[15] V. Tarokh, N. Seshadri and A. R. Calderbank, "Space-time codes for high data rate wireless communication: Performance criterion and code construction," *IEEE Trans. on Inf. Theory*, vol. 44, no. 2, pp.744-765, March 1998.

[16] E. Viterbo and E. Biglieri, "A universal lattice decoder," 14eme Colloque GRETSI, Juan-Les-Pins, pp. 611-614, September 1993.

[17] E. Viterbo and J. Boutros, "A universal lattice code decoder for fading channels," *IEEE Trans. on Inf. Theory*, pp. 1639-1642, July 1999.